Journal of Hydroscience and Hydraulic Engineering
Vol. 9, No. 2, January, 1992, 1-16

SAND BED INSTABILITY DUE TO NON-EQUILIBRIUM TRANSPORT OF SUSPENDED SEDIMENT

By

Tetsuro TSUJIMOTO

Associate Professor, Department of Civil Engineering, Kanazawa University
2-40-20, Kodatsuno, Kanazawa, 920, Japan

and

Tadanori KITAMURA

Graduate Student, Department of Civil Engineering, Kanazawa University
2-40-20, Kodatsuno, Kanazawa, 920, Japan

ABSTRACT

Sand-bed instability due to non-equilibrium suspended sediment is analyzed. Non-equilibrium concentration distribution of suspended sediment is described by using a convolution-integral model for turbulent flux distribution of suspended sediment of which impulse response is determined from the experimental data obtained in the transition process of the Reynolds-stress distribution of flow with abrupt change of bed roughness. The results reveals the effect of non-equilibrium suspended sediment on sand-bed instability, or sand-wave formation, by comparing them with those by the analysis based on non-equilibrium bed-load transport model previously conducted by Nakagawa & Tsujimoto.

INTRODUCTION

Kennedy (8) clarified that sand waves develop as a result of sand-bed instability and that the cause of sand-bed instability is the phase shift of sediment-transport rate from the bed geometry. This phase shift is composed of (i) phase lag of the bed shear stress to the bed geometry and (ii) the lag of sediment-transport rate to the bed shear stress. Since his paper, a lot of works have been done to evaluate (i) and (ii) quantitatively. Particularly as for the latter, Nakagawa & Tsujimoto (9) investigated it based on non-equilibrium bed-load transport model and evaluated it reasonably related to the step length of bed-load motion. In the case of suspended load, it is expected to take the excursion length instead of the step length of bed-load motion. Previously, Engelund & Fredsφe (1) analyzed sand-bed instability by taking account of the fact that the excursion length of suspended sediment is considerably long. The difference of sediment suspension from bed-load motion is, however, not only on the excursion length but on the concentration profile of suspended sediment is distorted along the flow depth and even the change of the sediment transport condition near the bed is somewhat influenced by the change of the concentration profile. Watanabe & Hirano (18) analyzed sand-bed instability by focussing on the non-equilibrium properties, but they hardly referred to whether their treatment of non-equilibrium sediment transport was certainly reasonable or not.

In this study, it is especially focussed on how to describe non-equilibrium transport of suspended sediment reasonably and in a simple mathematical form in order to conduct sand-bed instability analysis. The authors carried out a series of research which is necessary to be done before the present study. The summary is described below: (i) the proposal of relaxation model of turbulent-flux distribution due to the change of bed shear stress, which is prepared as a convolution-integral form with the impulse response; (ii) the determination of impulse response by using a wind-tunnel data of Jacobs (6) as for the investigation on the transition process of Reynolds-stress due to abrupt change of bed roughness; (iii) to confirm the applicability of the determined impulse-response function to an open-channel flow with abrupt change of bed roughness; (iv) to inspect the applicability of relaxation model to the various changing patterns of bed shear stress; (v) the application of the above model to the turbulent mass exchange of suspended sediment according to Reynolds' analogy; (vi) the deduction of non-equilibrium concentration profile of suspended sediment; and (vii) the experimental verification of the derived profile

in a sediment laden flow with spatial change of bed shear stress. The above (i), (ii) and (iii) are mentioned in Ref.(12). And (iv) was also inspected in Ref.(12) in case of open channel flow with monotonous increase of shear velocity. The applicability of the model to an open channel flow with higher Reynolds number was confirmed by field measurement of turbulence in Ref.(14), and the applicability to flows with cyclic changes of bed roughness such as a flow over a diffuse gravel sheet (a fluvial bed with longitudinally alternate sorting) was also inspected in Ref.(16). Furthermore, Ref.(15) treated (v), (vi) and (vii). Mathematical expressions required to the main purpose of the present paper are summarized in the following two chapters. If the non-equilibrium transport model is prepared, the sand-bed instability analysis can be conducted though several problems should be provisionally solved. In this paper, the analysis is proceeded being compared with the bed-instability analysis based on the non-equilibrium bed-load motion of Nakagawa & Tsujimoto (9). Thus, one can easily recognize the difference between sand bed instability due to suspension and that due to bed-load motion.

RELAXATION MODEL OF TURBULENT FLUX DISTRIBUTION

The response of the turbulent flux due to the change of the bed shear stress would be similar between the momentum and the mass. The turbulent flux would adapt the new condition faster near the bed and the response would delays more with distance from the bed. When the impulse response is known, the transition process of the turbulent flux distribution can be described as follows (12):

$$T(\eta\,|\xi) = \int_0^\infty T_e(\eta\,|\xi-\delta)\cdot g_R(\delta\,|\eta)\mathrm{d}\delta \tag{1}$$

in which $T(\eta\,|\xi)$=turbulent flux distribution at ξ; $\xi \equiv x/h$; x=longitudinal distance; $\eta \equiv y/h$; y=distance from the bed; h=flow depth in the case of open channel flow; $T_e(\eta\,|\xi)$=equilibrium turbulent flux distribution; and $g_R(\delta\,|\eta)$=impulse-response function of the turbulent flux at the relative height η. In the following, the subscript e indicates the values under equilibrium. The impulse-response function is often approximated by an exponential function as follows (12):

$$g_R(\xi\,|\eta\,) = \frac{1}{\Lambda(\eta)}\exp\left[-\frac{\xi}{\Lambda(\eta)}\right] \tag{2}$$

in which $\Lambda(\eta)$=relaxation scale made dimensionless by h at the relative height η.

In the case of the Reynolds-stress distribution ($\tau(\eta\,|\xi)$), its equilibrium profile is triangular, and thus Eq.1 is rewritten as

$$\tau(\eta\,|\xi) = (1-\eta)\int_0^\infty \tau_b(\xi-\delta)\cdot g_R(\delta\,|\eta)\mathrm{d}\delta \equiv (1-\eta)\cdot\tau_b(\xi)\cdot \Xi(\eta\,|\xi) \tag{3}$$

$$\Xi(\eta\,|\xi) \equiv \frac{\int_0^\infty \tau_b(\xi-\delta)\cdot g_R(\delta\,|\eta)\mathrm{d}\delta}{\tau_b(\xi)} = \int_0^\infty \psi_b(\xi-\delta)\cdot g_R(\delta\,|\eta)\mathrm{d}\delta \tag{4}$$

in which $\tau_b(\xi)$=bed shear stress at ξ; and $\psi_b(\xi-\delta)\equiv\tau_b(\xi-\delta)/\tau_b(\xi)$. $\Xi(\eta\,|\xi)$ represents the distortion of the Reynolds-stress profile from the equilibrium profile $(1-\eta)$. Applying the mixing length theory to the distorted Reynolds-stress profile, one can obtain the velocity distribution under non-equilibrium (12).

$\Lambda(\eta)$ was determined (Tsujimoto et al. (12)) as follows, according to the wind-tunnel data of Jacobs (6) which clarified the transition process of the Reynolds-stress distribution.

$$\Lambda(\eta) = 20\eta(1+1.5\eta^3) \tag{5}$$

When η=0, Λ=0 and then $g_R(\xi|0)$ becomes a delta function. It implies that $T(\eta|0)=T_e(\eta|0)$. Tsujimoto et al. (12) also confirmed the applicability of Eqs.2 and 5 to an open-channel flow by comparing them with the experimental data by Nezu et al. (11) which was obtained in open channel flows with an abrupt change of the bed roughness.

TURBULENT FLUX OF SUSPEDED SEDIMENT UNDER NON-EQUILIBRIUM

The turbulent momentum flux (the Reynolds stress) and the turbulent flux of suspended sediment are written as follows, respectively:

$$\tau = -\rho\overline{u'v'} = \rho\nu_T\frac{du}{dy}\ ; \qquad \Psi \equiv \overline{c'v'} = -\varepsilon_s\frac{dC}{dy} \tag{7}$$

in which u', v'=turbulence in the longitudinal and the vertical directions, respectively; ρ=mass density of fluid; ν_T=kinematic eddy viscosity (turbulent diffusion coefficient of momentum); u=velocity; C=concentration of suspended sediment; c'=fluctuation of suspended sediment concentration; and ε_s= turbulent diffusion coefficient of suspended sediment.

Considering the analogy between the mass exchange and the momentum exchange due to turbulence, one can write the following equation for the relaxation process of the turbulent flux of sediment with the same impulse response (15):

$$\Psi(\eta|\xi) = \int_0^\infty \Psi_e(\eta|\xi-\delta)\cdot g_R(\delta|\eta)d\delta \tag{8}$$

in which $g_R(\delta|\eta)$ is given by Eq.5; and the subscript e represents the values under equilibrium.

Under equilibrium, the upward flux of sediment by turbulence ($\overline{c'v'}$) must equal the downward flux by the terminal fall velocity ($C_e\nu_p$), and thus,

$$\Psi_e(\eta|\xi) = \nu_p\cdot C_e(\eta|\xi) \tag{9}$$

in which ν_p=terminal fall velocity of sediment. By applying Eq.7 to Eq.9, the equilibrium concentration profile of suspended sediment is obtained. When the diffusion coefficient of suspended sediment is identified with the depth-averaged value of the kinematic eddy viscosity ($\varepsilon_s=\kappa_0 u_* h/6$; κ_0=Kármán constant; u_*=shear velocity), the equilibrium concentration profile is obtained as follows:

$$\frac{C_e(\eta)}{C_{ae}} = \exp(-E\eta) \tag{10}$$

in which C_a=bottom concentration (C at η=0); and $E\equiv\nu_p h/\varepsilon_s=(6/\kappa_0)(\nu_p/u_*)$. Then,

$$\Psi_e(\eta|\xi) = C_{ae}\nu_p\exp(-E\eta) \tag{11}$$

As for the bottom concentration under equilibrium, a lot of works have been carried out, but still it is difficult to judge which formulation gives the best evaluation among them (see Nakagawa & Tsujimoto (10)). It can be expressed as a function of (ν_p/u_*) and $d^*\equiv(\sigma/\rho-1)gd^3/\nu^2$, in which σ=mass density of sediment; g=gravitational acceleration; ν=kinematic viscosity; and d=sediment diameter.

When the shear velocity varies spatially, we can rewrite Eq.8 as follows:

$$\Psi(\eta|\xi) = \nu_p\int_0^\infty C_{ae}(\xi-\delta)\cdot R(\xi-\delta)\cdot g_R(\delta|\eta)d\delta \tag{12}$$

in which $R(\eta\,|\xi)\equiv\exp[-E(\xi)\cdot\eta]$.

NON-EQUILIBRIUM CONCENTRATION PROFILE OF SUSPENDED SEDIMENT

When the turbulent flux of suspended sediment is estimated, its integration through the flow depth deduces a concentration profile as follows:

$$C(\eta\,|\xi) = -\frac{h}{\varepsilon_s(\xi)}\int_0^{\eta}\Psi(\zeta\,|\xi)\mathrm{d}\zeta + C(0\,|\xi) \tag{13}$$

Without determining the boundary condition at η=0 ($C(0\,|\xi)\equiv C_a(\xi)$), the following quantity can be calculated.

$$\Omega(\eta\,|\xi) \equiv \frac{C(\eta\,|\xi)-C_a(\xi)}{C_{ae0}} = -\frac{E}{C_{ae0}v_p}\int_0^{\eta}\Psi(\zeta\,|\xi)\mathrm{d}\zeta \tag{14}$$

in which the subscript 0 implies the undisturbed value.

The bottom boundary condition cannot be directly determined under non-equilibrium because of possible erosion and deposition. While, the boundary condition at $y=h$ (η=1) is easily obtained by the fact that a suspended particle cannot pass through the water surface, and that is,

$$v_pC_s(\xi) = \Psi(1\,|\xi) \tag{15}$$

in which $C_s(\xi)\equiv C(1\,|\xi)$. The right-hand side of Eq.15 has been already known by applying the relaxation model, as follows:

$$C_s(\xi) = \int_0^{\infty} C_{ae}(\xi-\delta)\cdot R_s(\xi-\delta)\cdot g_R(\delta\,|1)\mathrm{d}\delta \tag{16}$$

in which the subscript s implies the values at the water surface (η=1).

Non-equilibrium concentration distribution of suspended sediment is obtained as

$$\frac{C(\eta\,|\xi)}{C_{ae0}} = \Omega(\eta\,|\xi) - \Omega(1\,|\xi) + \frac{C_s(\xi)}{C_{ae0}} \tag{17}$$

The applicability of the above profile was verified in Ref.(15) by using the data of Yalin & Finlayson (17) and Kanda et al.(7).

The bottom concentration is obtained by setting η=0 in Eq.17, as follows:

$$\frac{C_a(\xi)}{C_{ae0}} = \frac{C_s(\xi)}{C_{ae0}} - \Omega(1\,|\xi) \tag{18}$$

v_pC_a implies the downward flux of sediment at the bottom. On the other hand, the upward flux is regarded as the turbulent flux of sediment at the bottom, and since this responds immediately to the local bed shear stress, it is expressed as v_pC_{ae}. The difference between the downward and the upward fluxes of sediment at the bottom brings about the variation of the bed elevation, and thus,

$$\frac{\partial z(x,t)}{\partial t} = v_p[C_a(x)-C_{ae}(x)] \tag{19}$$

FRAMEWORK OF BED INSTABILITY ANALYSIS

When the bed is undulated, the intensity of the flow and subsequently the sediment transport rate vary longitudinally, and the change of sediment transport rate brings the change of the bed geometry. In other words, an interacted closed system takes place. Sand-wave formation can be treated as an instability analysis of this system (Kennedy (8)). Particularly, when a linear approximation is allowed, the initial small disturbance of the bed elevation (z), which is sinusoidal (Fig.1), brings about the small sinusoidal perturbation of $\partial z/\partial t$ through the interaction of the system, as written by

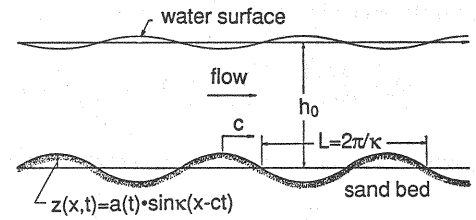

Fig.1 Definition sketch

$$z(x,t) = a \cdot \sin\kappa(x-ct) \tag{20}$$

$$\frac{\partial z}{\partial t} = a r_T \sin[\kappa(x-ct)-\phi_T] \tag{21}$$

in which a=amplitude of bed undulation; κ=angular wave number ($=2\pi/L$; L=wave length); c= propagation celerity of the disturbance; and ar_T, ϕ_T=amplitude and phase shift of the perturbation of $\partial z/\partial t$ from z, respectively. Comparing Eq.21 with the time derivative of Eq.20, we obtain the following relations:

$$\frac{1}{a}\frac{\partial a}{\partial t} = r_T \cos\phi_T \; ; \quad c\kappa = r_T \sin\phi_T \tag{22}$$

Eq.22 implies that one can judge whether the disturbance grows or decays and which direction it propagates if one can evaluate the phase shift ϕ_T, as shown in Table 1.

Table 1 Behavior of the bed disturbance

quadrature of ϕ_T	behavior of bed disturbance	
1	unstable	moving downstream
2	stable	moving downstream
3	stable	moving upstream
4	unstable	moving upstream

LINEARIZATION OF GOVERNING EQUATIONS

When the bed is undulated as written by Eq.20, the shear velocity varies in general with lag. It is to be described as follows in a linearized mode:

$$u_*(x,t) = u_{*0}\{1+r_f a \cdot \sin[\kappa(x-ct)-\phi_f]\} \tag{23}$$

in which $r_f a u_{*0}$, ϕ_f=amplitude of the perturbation of the shear velocity and its phase shift from the bed geometry, respectively; and the subscript 0 indicates the undisturbed values. r_f and ϕ_f are evaluated by an appropriate model of flow over a wavy bed. In the following, the dimensionless perturbation of the shear velocity is represented by ω_f as follows:

$$\omega_f \equiv r_f a \cdot \sin[\kappa(x-ct)-\phi_f] \equiv r_f a \cdot \sin\Theta \tag{24}$$

E and C_{ae} in Eq.10 are functions of the shear velocity, and thus the perturbations of E and C_{ae} normalized by their respective undisturbed values, ω_E and ω_{cae}, can be related to ω_f as follows under linear approximation:

$$\omega_E = \frac{\partial E}{\partial u_*}\Big|_0 \frac{u_{*0}}{E_0}\cdot\omega_f = -\omega_f \quad ; \qquad \omega_{cae} = \frac{\partial C_{ae}}{\partial u_*}\Big|_0 \frac{u_{*0}}{C_{ae0}}\cdot\omega_f \equiv A(u_{*0})\cdot\omega_f \tag{26}$$

Moreover, the dimensionless perturbation of R involved in Eqs.12 and 16, ω_R, is expressed as follows:

$$\omega_R = \frac{\partial R}{\partial u_*}\Big|_0 \frac{u_{*0}}{R_0}\cdot\omega_f = E_0\eta\cdot\omega_f \tag{27}$$

Then, Eqs.12 and 16 are rewritten as follows:

$$\begin{aligned}\frac{\Psi(\eta\,|\xi)}{C_{ae0}v_p} &= R_0(\eta)\int_0^\infty [1+(A+E_0\eta)\omega_f(\xi-\delta)]\cdot g_R(\delta\,|\eta)\mathrm{d}\delta \\ &= R_0(\eta)\Big[1+(A+E_0\eta)\int_0^\infty \omega_f(\xi-\delta)\cdot g_R(\delta\,|\eta)\mathrm{d}\delta\Big]\end{aligned} \tag{28}$$

$$\frac{C_s(\xi)}{C_{ae0}} = R_{0s}\int_0^\infty [1+(A+E_0)\omega_f(\xi-\delta)]\cdot g_R(\delta\,|1)\mathrm{d}\delta = R_{0s}\Big[1+(A+E_0)\int_0^\infty \omega_f(\xi-\delta)\cdot g_R(\delta\,|1)\mathrm{d}\delta\Big] \tag{29}$$

By using Eq.28, $\Omega(1\,|\xi)$ is expressed as

$$\begin{aligned}\Omega(1\,|\xi) &= -E_0\int_0^1 R_0(\eta)\Big[1+(A+E_0\eta)\int_0^\infty \omega_f(\xi-\delta)\cdot g_R(\delta\,|\eta)\mathrm{d}\delta\Big]\mathrm{d}\eta \\ &= -E_0\Big[\int_0^1 R_0(\eta)\mathrm{d}\eta + \int_0^1 (A+E_0\eta)R_0(\eta)\int_0^\infty \omega_f(\xi-\delta)\cdot g_R(\delta\,|\eta)\mathrm{d}\delta\Big]\mathrm{d}\eta \\ &= -1 + R_{0s} - E_0\int_0^1 (A+E_0\eta)R_0(\eta)\int_0^\infty \omega_f(\xi-\delta)\cdot g_R(\delta\,|\eta)\mathrm{d}\delta\mathrm{d}\eta\end{aligned} \tag{30}$$

Then, the bottom concentration is expressed as follows:

$$\frac{C_a(\xi)}{C_{ae0}} = 1 + R_{0s}(A+E_0)\omega_r(\xi\,|1) + E_0\int_0^1 (A+E_0\eta)R_0(\eta)\omega_r(\xi\,|\eta)\mathrm{d}\eta \tag{31}$$

in which

$$\omega_r(\xi\,|\eta) \equiv \int_0^\infty \omega_f(\xi-\delta)\cdot g_R(\delta\,|\eta)\mathrm{d}\delta \tag{32}$$

When the shear velocity has a sinusoidal perturbation (ω_f) as written in Eq.23 or Eq.24, $\omega_r(\xi\,|\eta)$ is calculated as follows by using the impulse-response function given by Eq.2:

$$\omega_r(\xi\,|\eta) = r_r(\eta)\cdot a r_f\cdot\sin[\Theta-\phi_r(\eta)] = a r_f\big[B_2(\eta)\cdot\sin\Theta - B_1(\eta)\cdot\cos\Theta\big] \tag{33}$$

in which

$$B_1(\eta)\equiv r_r(\eta)\cdot\sin[\phi_r(\eta)]=\frac{\kappa^*\Lambda(\eta)}{1+[\kappa^*\Lambda(\eta)]^2};\qquad B_2(\eta)\equiv r_r(\eta)\cdot\cos[\phi_r(\eta)]=\frac{1}{1+[\kappa^*\Lambda(\eta)]^2} \tag{34}$$

and $\kappa^*\equiv\kappa h_0$ (h_0=undisturbed flow depth). $\Lambda(\eta)$ is given by Eq.5.

The dimensionless perturbation of C_a, ω_{ca}, is written by

$$\omega_{ca} = ar_f[K_2\sin\Theta - K_1\cos\Theta] = ar_f r_{ca}\sin(\Theta-\phi_{ca}) \tag{35}$$

in which

$$r_{ca}\sin\phi_{ca} = K_1 \equiv R_{0s}(A+E_0)B_{1s} + E_0\int_0^1 (A+E_0\eta)R_0(\eta)B_1(\eta)d\eta\ ;$$
$$r_{ca}\cos\phi_{ca} = K_2 \equiv R_{0s}(A+E_0)B_{2s} + E_0\int_0^1 (A+E_0\eta)R_0(\eta)B_2(\eta)d\eta \tag{36}$$

Substituting Eqs.26 and 36 into Eq.19, we obtain the following equation.

$$\frac{\partial z}{\partial t} = \nu_p C_{ae0}(\omega_{ca}-\omega_{cae}) = ar_f\nu_p C_{ae0}[(K_2-A)\sin\Theta - K_1\cos\Theta]$$
$$= ar_f\nu_p C_{ae0} r_{zt}\sin(\Theta-\phi_{zt}) = ar_T\sin(\Theta-\phi_{zt}) \tag{37}$$

in which

$$r_{zt}\sin\phi_{zt} = K_1\ ;\qquad r_{zt}\cos\phi_{zt} = K_2 - A \tag{38}$$

and $ar_T\equiv a\nu_p C_{ae0} r_{zt} r_f$, ϕ_{zt}=amplitude of the perturbation of $\partial z/\partial t$ and its phase shift from the perturbation of the shear velocity (ω_f), respectively. The phase shift of $\partial z/\partial t$ from the bed geometry (z) is given as $\phi_T=\phi_{zt}+\phi_f$, and thus,

$$r_{zt}\sin\phi_T = K_1\cos\phi_f + (K_2-A)\sin\phi_f\ ;\qquad r_{zt}\cos\phi_T = -K_1\sin\phi_f + (K_2-A)\cos\phi_f \tag{39}$$

When Eq.22 is applied, the behavior of the bed disturbance is characterized by the following equations:

$$M^* \equiv \frac{h_0}{\nu_p a}\frac{\partial a}{\partial t} = r_T\cos\phi_T = C_{ae0}[-K_1 r_{f*}\sin\phi_f + (K_2-A)r_{f*}\cos\phi_f] \tag{40}$$

$$N^* \equiv \frac{c}{\nu_p} = r_T\sin\phi_T = \frac{C_{ae0}}{\kappa^*}[K_1 r_{f*}\cos\phi_f + (K_2-A)r_{f*}\sin\phi_f] \tag{41}$$

in which $r_{f*}\equiv r_f h_0$ (dimensionless). E_0, R_0 and A are in general expressed as functions of (u_{*0}/ν_p) for the constant sediment properties. B_1 and B_2 are functions of κ^*. Thus, K_1 and K_2 are functions of (u_{*0}/ν_p) and κ^*. Meanwhile, $r_{f*}\sin\phi_f$ and $r_{f*}\cos\phi_f$ might be functions of κ^* and the flow parameters such as the Froude number and the relative depth.

MODELS FOR FLOW OVER WAVY BED AND SEDIMENT ENTRAINMENT

When ϕ_T is evaluated, one can judge the stability of the bed for non-equilibrium suspended sediment transport. The problems which remain to be resolved are (i) to establish a model for flow over a wavy bed to determine ϕ_f; and (ii) to establish a model to estimate the equilibrium bottom concentration C_{ae0} and to evaluate $A(u_{*0})$.

Model of Flow over a Wavy Bed:

For the problem (i), turbulent shear flow model has succeeded in shear flow analysis (see Ref.(10) for example) though the earlier studies adopted a potential flow model or a one-dimensional flow model. In this paper, a model proposed by Nakagawa & Tsujimoto (9), which is never a rigorous flow model in these days but by which the bed instability due to bed-load motion is analyzed, is adopted, in order to compare the effect of non-equilibrium sediment suspension on sand-bed instability with that of non-equilibrium bed-load motion. The following resistance law is assumed here:

$$\tau_b(x) = \beta_f \rho U^2 \left(1 - \frac{\gamma_2 \partial h}{Fr^2 \partial x}\right) \tag{42}$$

in which U=representative flow velocity; β_f=resistance coefficient; and γ_2=empirical constant. In the above, the effect of the spatial acceleration was taken into account. A similar expression was already adopted in Hayashi's analysis (3). When the flow depth and the representative velocity are assumed to be given by the potential flow model over a wavy bed (Kennedy (8)), the dimensionless perturbation of the bed shear stress, ω_τ, which is twice ω_f because $u_* \sim \sqrt{\tau_b}$, is expressed as follows:

$$\omega_\tau = 2\omega_f = 2 r_f a \cdot \sin[\kappa(x - ct) - \phi_f] \tag{43}$$

$$r_{f*} \sin\phi_f = \frac{\gamma_2 \kappa^* (R^* - 1)}{2Fr^2}; \qquad r_{f*} \cos\phi_f = \kappa^* F^* \tag{44}$$

$$R^* = \frac{Fr^2 \kappa^* \operatorname{sech}\kappa^*}{Fr^2 \kappa^* - \tanh\kappa^*}; \qquad F^* = \frac{1 - Fr^2 \kappa^* \tanh\kappa^*}{\tanh\kappa^* - Fr^2 \kappa^*} \tag{45}$$

in which $Fr \equiv U_0/\sqrt{g h_0}$=Froude number of the undisturbed flow. Without the effect of the spatial acceleration, γ_2=0 and the shear velocity and the flow velocity are in phase, and ϕ_f is 0 or π.

Model for Sediment Entrainment from a Bed:

For the problem (ii), the following empirical formula is adopted here:

$$C_{ae} = \alpha \left(\frac{u_*}{v_p}\right)^m \left[1 - \beta_c \left(\frac{v_p}{u_*}\right)^2\right]^n \tag{46}$$

in which α, m, n=empirical constants ($\alpha \cong 0.002$ $m \cong 2$; $n \cong 1.5$ according to the previous experimental data, see Nakagawa & Tsujimoto (10)); $\beta_c \equiv (u_{*c}/v_p)^2$; and u_{*c}=critical shear velocity. β_c depends on $d^* \equiv (\sigma/\rho - 1) g d^3/\nu^2$. Then, Eq.26 provides an expression for A as follows:

$$A = m + 2n\beta_c \left[\left(\frac{u_*}{v_p}\right)^2 - \beta_c\right]^{-1} \tag{47}$$

If the argument is limited to the range where (u_*/v_p) is sufficiently larger than β_c, $A=m$. As for the critical tractive force, Iwagaki's formula (5) is familiar, and it can be approximated by the following equation (Tsujimoto & Saito (15)).

$$\sqrt{\beta_c}=\frac{u_{*c}}{v_p}=(0.0455d^*)^{-0.65}+0.25 \tag{48}$$

in which Rubey's formula (see Ref.(10) for example) has been used to determine the terminal fall velocity.

RESULT OF INSTABILITY ANALYSIS

When the above-mentioned models of flow and sediment entrainment are provisionally adopted, the dimensionless growth rate and propagation celerity of the perturbation are written as follows:

$$M^{**}\equiv\frac{M^*}{C_{ae0}}\equiv\frac{h_0}{C_{ae0}v_p a}\frac{\partial a}{\partial t}=\left[-\frac{K_1\gamma_2(R^*-1)}{2Fr^2}+(K_2-A)F^*\right]\kappa^* \tag{49}$$

$$N^{**}\equiv\frac{N^*}{C_{ae0}}\equiv\frac{c}{v_pC_{ae0}}=K_1F^*+\frac{(K_2-A)\gamma_2(R^*-1)}{2Fr^2} \tag{50}$$

The singularity, which makes the denominators of Eq.49 or Eq.45 zero, is expressed by the following relation, which is often termed "Airy's relation."

$$Fr^2=\frac{\tanh\kappa^*}{\kappa^*} \tag{51}$$

Eq.51 gives the critical Froude number, and if the Froude number is smaller than it, the flow is in the lower regime; otherwise in the upper regime.

The neutral stability ($M^*=0$) is given by the following relation.

$$D_1Fr^4-D_2Fr^2+D_3=0 \tag{52}$$

$$D_1=2(K_2-A)\kappa^*\tanh\kappa^*\ ;\quad D_2=K_1\gamma_2\kappa^*(\mathrm{sech}\,\kappa^*-1)+2(K_2-A)\ ;\quad D_3=-K_1\gamma_2\tanh\kappa^* \tag{55}$$

Thus,

$$Fr^2=\frac{D_2\pm\sqrt{D_2^2-4D_1D_3}}{2D_1} \tag{56}$$

When $(D_2^2-4D_1D_3)<0$, the neutral relation does not exist; and when the right-hand side of Eq.56 is negative, such a relation is meaningless. Eqs.51 and 56 represent the borders which distinguish unstable regions from stable ones.

The relation which corresponds to $N^*=0$ (stationary disturbance) is expressed as follows:

$$D_4Fr^4-D_5Fr^2+D_6=0 \tag{57}$$

$$D_4=2K_1\kappa^*\tanh\kappa^*\ ;\qquad D_5=2K_1-[(K_2-A)\gamma_2\mathrm{sech}\,\kappa^*-]\kappa^*\ ;\qquad D_6=(K_2-A)\gamma_2\tanh\kappa^* \tag{60}$$

Thus,

$$Fr^2=\frac{D_5\pm\sqrt{D_5^2-4D_4D_6}}{2D_4} \tag{61}$$

When $(D_5^2-4D_4D_6)<0$, no relation exists where $N^*=0$; and when the right-hand side of Eq.61 is negative, such a relation is meaningless. Eqs.51 and 61 represent the borders at which the propagation celerity of the disturbance changes the sign.

Phase Shift of $\partial z/\partial t$ from the Shear Velocity, ϕ_{zt}:

The phase shift ϕ_{zt} has been calculated by Eq.38 with the aid of Eqs.34 and 35. On calculation, it has been assumed that $\beta_c=0.8$, which corresponds to the sediment whose diameter is almost 0.5mm. The calculated values of ϕ_{zt} are plotted against κ^* with u_{*0}/v_p as a parameter in Fig.2. ϕ_{zt} increases with κ^* monotonously from 0 to π; that is, ϕ_{zt} varies in the 1st quadrature in the range of lower wave number, and then varies in the 2nd in the range of higher wave number. ϕ_{zt} increases more gradually with κ^* for the smaller value ofu_{*0}/v_p, while more rapidly approaches to π for the larger value of u_{*0}/v_p.

The dashed curves in Fig.2 are the results in the case of non-equilibrium bed-load transport (Nakagawa & Tsujimoto (9)), in which Λ_B represents the mean step length of bed load. The dashed curve (e) corresponds to $\Lambda_B/h_0=1.0$ and (f) to $\Lambda_B/h_0=10$. Since the mean step length is roughly proportional to the sand diameter, $\gamma_1\equiv\Lambda_B/h_0$ increases with the relative submergence (h_0/d). In the case of bed-load motion, $\partial z/\partial t$ is expressed as a difference of the deposition rate to the pick-up rate instead of Eq.19. When the perturbation of the pick-up rate is expressed as a sinusoidal curve, that of the deposition rate becomes a sinusoidal curve with the same amplitude and the phase shift belonging to the 1st quadrature. Then, the phase shift of $\partial z/\partial t$ from the perturbation of the pick-up rate belongs to the 2nd quadrature. In the case of suspended sediment, on the other hand, $\partial z/\partial t$ is expressed as the difference between C_a and C_{ae}, and C_a has a phase shift belonging to the 1st quadrature and the different (suppressed) amplitude against C_{ae}. Hence, the cosine of ϕ_{zt} is not always positive while its sine is always positive, and thus ϕ_{zt} belongs to the 1st or the 2nd quadrature. This study emphasizes that the sand-bed instability due to a non-equilibrium suspended sediment cannot be explained by the model for bed-load transport even if one simply replaces the step length of bed-load motion by the larger excursion length of suspension.

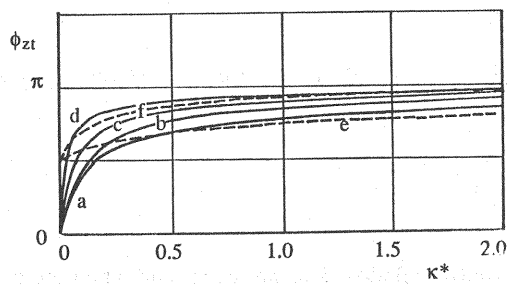

(a) u_{*0}/v_p= 1.0 ; (b) u_{*0}/v_p= 3.0; (c) u_{*0}/v_p= 5.0; (d) u_{*0}/v_p=10.0
----- non-equilibrium bed-load model: (e) Λ_B/h_0=1.0; (f) Λ_B/h_0=10
(Λ_B=mean step length)

Fig.2 Phase shift between $\partial z/\partial t$ and shear velocity, ϕ_{zt}

Phase Shift of the Shear Velocity from the Bed Geometry, ϕ_f:

The calculated result of Eq.44 is shown in Fig.3, which was already published by Nakagawa & Tsujimoto (9). The parameter γ_2 was set 1.0. The figure suggests that ϕ_f decreases against κ^* from zero and belongs to the 4th quadrature in the case of the lower regime; while it is nearly π in the case of the upper regime unless the flow depth is out of phase to the bed geometry ($R^*>1$ for relatively lower wave number range), otherwise it is nearly zero.

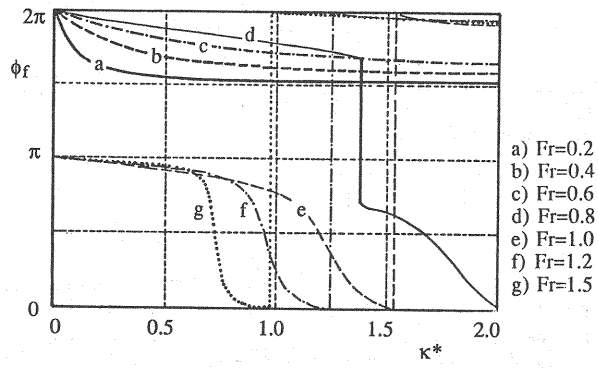

Fig.3 Phase shift between shear velocity and bed geometry, ϕ_f

Phase Shift of $\partial z/\partial t$ from the Bed Geometry, ϕ_{zt}, and Bed Instability:

The sum of the phase shifts ϕ_f and ϕ_{zt} provides the phase shift of $\partial z/\partial t$ from the bed geometry, ϕ_T, and it is used for judgement of the bed instability (see Table 1). The calculated value of ϕ_T is shown against κ^* with Fr and u_{*0}/v_p as parameters in Fig.4. In the lower regime, ϕ_T may belong to the 1st quadrature for relatively lower wave number range ($\kappa^* <\fallingdotseq 1.0$), and it corresponds to unstable bed disturbance propagating downstream. On the other hand, in the upper regime, ϕ_T may belong to the 4th quadrature for the relatively lower wave number range, and bed disturbance falls unstable propagating upstream. For the relatively higher wave number range, ϕ_T may belong to the 2nd quadrature.

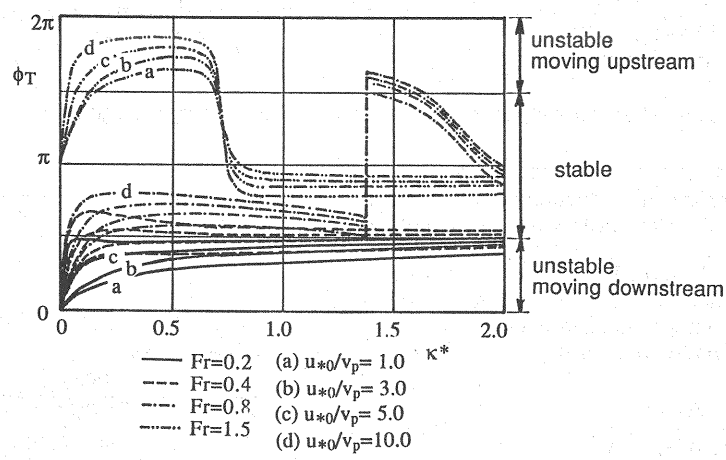

Fig.4 Phase shift between $\partial z/\partial t$ and bed geometry, ϕ_T

Now that the quadrature which ϕ_T belongs to is known, the regions are divided in the Fr~κ^* plane according to whether the disturbance is unstable or stable as shown in Fig.5. The borders of the regions are expressed by Eqs.51 and 56. In Fig 6 is shown the result of Nakagawa & Tsujimoto (9) for bed-load motion, which is consistent to the result by Hayashi (3). In Fig.6(a), unstable region in Fr~κ^* is shown (while Fig.6(b), propagating directions are shown; and in Fig.6(c) unstable regions are compared with the observed data). Comparing Fig.5 with Fig.6, one can see that the present result has different aspects from the results based on bed-load transport model as follows: In the lower regime, disturbances with the wave number near the wave number which satisfies the Airy's relation are stable, and thus the lower-regime unstable disturbance, or lower-regime bed-forms have relatively low wave number when the Froude number is relatively high (but of course smaller than the critical Froude number). In the upper regime, disturbances with extremely low wave number are stable.

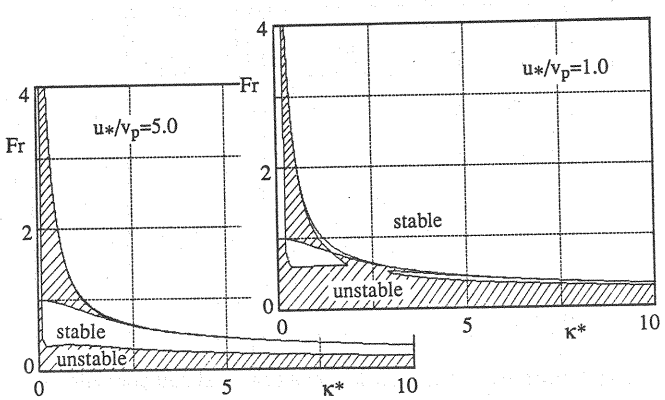

Fig.5 Unstable region in Fr~κ^* plane based on the present model for suspended sediment

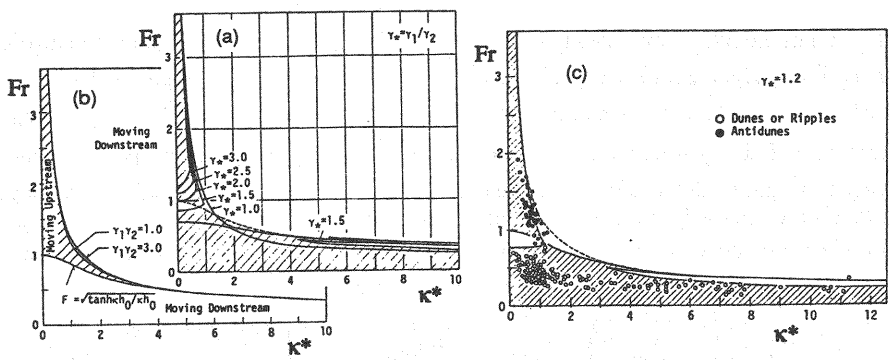

Fig.6 Results of bed instability analysis based on bed-load model by Nakagawa & Tsujimoto

The regions are divided in Fr~κ^* plane according to the propagation direction of disturbance as shown in Fig.7. The borders are expressed by Eqs.51 and 61.

Equation 51 and the following equation represent the borders between the region where the flow depth is in phase to the bed geometry and that where it is out of phase to the bed.

$$Fr^2 = \frac{\tanh\kappa^*}{\kappa^*(\mathrm{sech}\,\kappa^* - 1)} \qquad (62)$$

The change of the dimensionless growth rate of disturbance (M^{**}) against the wave number with Fr as a parameter is shown for two different values of (u_{*0}/v_p) in Fig.8. (u_{*0}/v_p) represents the predominance of suspension compared with bed-load motion, and the relation among M^{**}, κ^* and Fr changes with this parameter obviously. M^{**} has a maximum at a certain value of κ^* under a constant value of Fr. The dimensionless wave number corresponding to such a maximum growth rate (κ^*_p) is shown as a function of the Froude number in Fig.9. This relation would estimate the predominant wave length of sand waves when suspended sediment dominates.

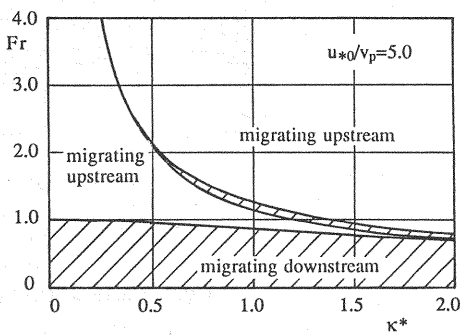

Fig.7 Propagating direction of disturbance

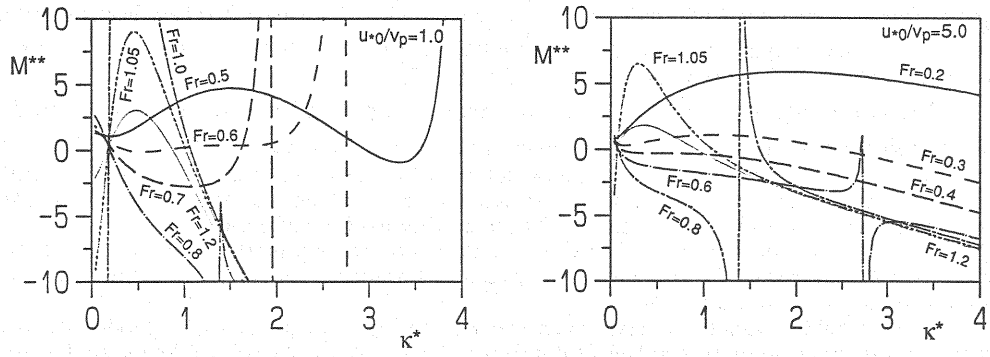

Fig.8 Growth rate of bed disturbance due to non-equilibrium suspended load

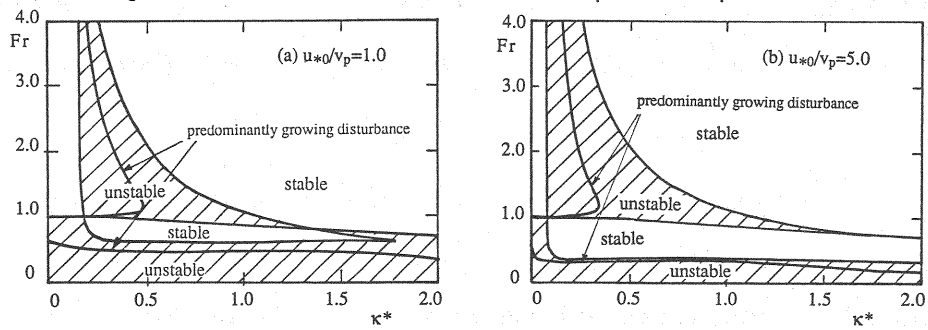

Fig.9 Predominant wave length defined by maximum growth rate

CONCLUSIONS

The results obtained in this study are summarized below:

(1) When the suspended sediment is predominant, the bed deformation is expressed as the difference between the upward turbulent flux of sediment and the downward flux due to fall velocity at the bottom. For the spatial change of the shear velocity, the turbulent flux responds immediately at the bed but the relaxation distance of the response of the turbulent flux increases with the distance from the bed. It implies that the upward flux responds to the bed shear instantaneously.

(2) Applying the relaxation model of the turbulent flux with the concept of impulse response, the non-equilibrium profile of turbulent sediment flux can be estimated. The impulse response has been determined by the investigation of the transition process of the Reynolds-stress (turbulent flux of momentum of the water) of flow with an abrupt change of the bed roughness.

(3) By integrating the turbulent flux profile of suspended sediment, the concentration distribution is obtained. The boundary condition is given at the water surface based on the following fact: Even under non-equilibrium, the (upward) turbulent flux of sediment is equivalent to the downward flux expressed by the product of the fall velocity and the concentration at the water surface.

(4) From the boundary condition at the water surface and the calculated turbulent flux of sediment, one can estimate the non-equilibrium bottom concentration. The product of it with the fall velocity gives the downward flux of sediment at the bottom.

(5) When the spatial change of the shear velocity of the flow is expressed by a sinusoidal wave with a small amplitude, the phase lags and the amplitudes of the perturbations of the responding equilibrium and non-equilibrium bottom concentrations are deduced as functions of the wave number and the shear velocity. The amplitudes of these two are different. The phase shift of the equilibrium bottom concentration has the same phase with the shear velocity but that of the non-equilibrium bottom concentration is larger than that of shear velocity by the phase belonging to the 1st quadrature. As a result, the phase shift of the time derivative of the bed elevation ($\partial z/\partial t$) from the shear velocity, ϕ_{zt}, belongs to the 1st or the 2nd quadrature.

(6) The effect of the spatial derivative of the flow depth has been taken into account in the relation between the shear velocity and the representative flow velocity. By applying the potential flow model,

the spatial change of the flow depth and the representative velocity over a wavy bed have been estimated. As a result, the phase shift of the shear velocity from the bed geometry, ϕ_f, is estimated as a function of the wave number and the Froude number of the undisturbed flow.

(7) The phase shift between $\partial z/\partial t$ and the bed geometry, ϕ_T, has been evaluated as $\phi_{zt}+\phi_f$. The linear instability analysis reveals the relation between the behavior of the bed disturbance and ϕ_T. The growth rate of the amplitude and the propagation celerity of the bed disturbance have been evaluated against the wave number with the Froude number and the shear velocity as parameters. The relation between the predominant wave number and the Froude number has been also deduced.

(8) The difference of the results based on the theory of non-equilibrium suspended sediment transport from those based on the non-equilibrium bed-load transport model has been pointed out, but it has not yet confirmed by the flume data.

Sand-bed instability usually observed is caused not only by non-equilibrium suspended sediment transport but also by non-equilibrium bed-load transport. In this study, the role of the former has been separately treated. Sand bed instability due to a combination of the both transports should be inspected as the next step of research.

The basic idea and the outline of the analysis were already published in Ref.(13) in Japanese.

REFERENCES

1. Engelund, F. and J. Fredsφe : Transition from dunes to plane bed in alluvial channels, *Series Paper*, 4, ISVA, Technical University of Denmark, 1974.
2. Fredsφe, J. : On the development dunes in erodible-channels, *Jour. Fluid Mech.*, Vol.64, Part 1, pp.1-16, 1974.
3. Hayashi, T. : Formation of dunes and antidunes in open channels, *Jour. Hydraul. Div.*, ASCE, Vol.96, HY2, pp.357-366, 1970.
4. Hayashi, T. and M. Onishi : Dominant wave numbers of ripples, dunes and antidunes on alluvial river beds, *Proc. 2nd Int. Sym. River Sedimentation*, Nanjing, China, pp.472-481, 1983.
5. Iwagaki, Y. : Hydrodynamic study on critical tractive force, *Trans. JSCE*, No.41, pp.1-21, 1956 (in Japanese).
6. Jacobs, W. : Umformung eines turbulenten Geschwindigkeits-Profils, *Z. Angew. Math. und Mech.*, 19, pp.87-100, 1939 (see*"Boundary-Layer Theory"*, 6th edition by H. Schlichting, pp.615-616, McGraw-Hill, 1968).
7. Kanda, K., Y. Muramoto, Y. Fujita and T. Yada : Transition process of turbulent structure and suspended sediment concentration in open channel with sudden bottom roughness change, *Annuals*, Disas. Prev. Res. Inst., Kyoto Univ., No.32B-2, pp.619-639, 1989 (in Japanese).
8. Kennedy, J.F. : The mechanics of dunes and antidunes in erodible-bed channels, *Jour. Fluid Mech.*, Vol.16, Part 4, pp.521-544, 1963.
9. Nakagawa, H. and T. Tsujimoto : Sand bed instability due to bed load motion, *Jour. Hydraul. Div.*, ASCE, Vol.106, HY12, pp.2029-2051, 1980.
10. Nakagawa, H. and T. Tsujimoto : *Mechanics of Sediment Transport and Hydraulics in Alluvial Channels*, Gihodo Shuppan, 350p., 1986 (in Japanese).
11. Nezu, I., H. Nakagawa, K. Seya and Y. Suzuki : Response of velocity distribution and bed shear stress of open channel flow with abrupt change of bed roughness, *Proc. Hydraul. Eng.*, JSCE,Vol.34, pp.505-510, 1990 (in Japanese).
12. Tsujimoto, T., H.A. Cardoso and A. Saito : Open channel flow with spatially varied bed shear stress, *Jour. Hydroscience & Hydraul. Engrg.*, JSCE, pp.1-20, Vol.8, No.2, pp.1-25, 1990.
13. Tsujimoto, T. and T. Kitamura : Sand bed instability due to non-equilibrium suspended sediment transport, *Proc. Hydraul. Eng.*, JSCE, Vol.35, pp.371-376, 1990 (in Japanese).
14. Tsujimoto, T., T. Kitamura, T. Okada and Y. Ouji : Field measurements of turbulent flow in channels and rivers, *KHL-Commun.*, Kanazawa Univ., No.2, pp.107-120, 1991.
15. Tsujimoto, T. and A. Saito : Non-equilibrium profile of suspended sediment concentration, *Jour. Hydroscience & Hydraul. Engrg.*, JSCE, pp.1-20, Vol.9, No.1, pp.49-61, 1991.
16. Tsujimoto, T., M. Urushizaki and K. Miyagaki : Turbulent flow with abrupt changes of bed roughness in open channels, *KHL-Commun.*, Kanazawa Univ., No.2, pp.59-78, 1991.
17. Yalin, M.S. and G.D. Finlayson : On the development of the distribution of suspended load, *Proc. 16th IAHR Cong.*, Istanbul, Turkey, Vol.1, pp.287-294, 1973.

18. Watanabe, K. and M. Hirano : Effect of suspended sediment on formation of sand waves, *Jour. Hydroscience & Hydraul. Engrg.*, JSCE, pp.1-25, Vol.6, No.2, pp.29-42, 1990.

APPENDIX - NOTATION

The following symbols are used in this paper:

a	= amplitude of bed-surface disturbance;
A	= defined by Eq.47;
B_j	= defined in Eq.34 (j=1, 2);
c	= propagation celerity of perturbation;
C, c'	= concentration distribution of suspended sediment and its fluctuation;
C_a, C_a	= concentration of suspended sediment at bottom and at water surface, respectively;
d	= sediment diameter;
d^*	$\equiv (\sigma/\rho-1)gd^3/\nu^2$;
D_j	= defined by Eqs.55 and 60 (j=1~6);
E	$\equiv v_p h/\varepsilon_S$;
F^*	= defined by Eq.45;
Fr	$\equiv U_0/\sqrt{gh_0}$ = Froude number of undisturbed flow;
g	= gravitational acceleration;
$g_R(\delta \mid \eta)$	= impulse response of turbulent flux at the relative height η;
h	= depth of flow;
K_j	= defined in Eq.36 (j=1, 2);
L	= wave length of bed undulation;
m, n	= empirical constants in Eq.46;
M^*, M^{**}	= dimensionless growth rate of perturbation defined in Eqs.40 and 49, respectively;
N^*, N^{**}	= dimensionless propagation celerity of perturbation defined in Eqs.41 and 50, respectively;
r_Q	= ratio of amplitude of the perturbation of the quantity Q to that of bed geometry;
r_{f*}	$= r_f h_0$;
R	$\equiv \exp(-E\eta)$;
R^*	= defined by eq.45;
t	= time;
T	= turbulent flux;
u, U	= local velocity and depth-averaged velocity;
u_*, u_{*c}	= shear velocity and critical shear velocity;
u', v'	= turbulence in longitudinal and vertical directions;
v_p	= terminal velocity of sand;
x	= longitudinal distance;
y	= height from the bed;
z	= height of bed surface from the mean bed level;

α = empirical constant in Eq.46;

β_c $\equiv u_{*c}/\nu_p$;

β_f = a kind of resistance coefficient;

γ_1 $\equiv \Lambda_B/h_0$;

γ_2 = empirical constant in Eq.42;

$\Gamma(\eta|\zeta)$ = deviation of turbulent flux under non equilibrium from equilibrium one and defined in Eq.4;

ε_s = diffusion coefficient of suspended sediment;

η $\equiv y/h$ = relative height;

Θ $\equiv \kappa[(x-ct)-\phi_f]$;

κ, κ^* = angular wave number and its dimensionless version (κh_0);

κ_0 = Kármán constant;

$\Lambda(\eta)$, Λ_s = relaxation scale non-dimensionalized by h at η and its value at the surface;

Λ_B = step length of bed load;

ν, ν_T = kinematic viscosity and eddy kinematic viscosity;

ξ $\equiv x/h$;

Ξ = dimensionless change of bed shear stress defined by Eq.4;

ρ, σ =mass density of water and mass density of sand;

τ = Reynolds stress;

τ_b = bed shear stress;

τ_*, τ_{*b} = dimensionless bed shear stress and dimensionless critical tractive force;

ϕ_Q = phase shift of the quantity Q from the bed geometry;

$\psi_b(\xi-\delta)$ $\equiv \tau_b(\xi-\delta)/\tau_b(\xi)$;

Ψ = turbulent flux of suspended sediment;

ω_Q = dimensionless perturbation of the quantity Q; *and*

$\Omega(\eta)$ = defined by Eq.14.

Subscripts:

e = values under equilibrium conditions;

f = values with respect to the perturbation of shear velocity;

s = values at the water surface;

T = values with respect to $\partial z/\partial t$ and z;

zt = values with respect to $\partial z/\partial t$ and shear velocity;

0 = undisturbed values.

(Received July 26, 1991; revised December 6, 1991)